Study of Structural Phase Transitions in $[Mg(H_2O)_6][SiF_6]$ by Means of Single Crystal ^{2}H NMR

Takahiro Iijima, Motohiro Mizuno, Masahiko Suhara, and Kazunaka Endo
Department of Chemistry, Faculty of Science, Kanazawa University, Kanazawa 920-1192, Japan
Reprint requests to Dr. M. M.; E-mail: mizuno@wriron1.s.kanazawa-u.ac.jp

Z. Naturforsch. **57 a,** 408–412 (2002); received February 26, 2002

Presented at the XVIth International Symposium on Nuclear Quadrupole Interactions, Hiroshima, Japan, September 9-14, 2001.

The temperature and angular dependences of ^{2}H NMR spectra were measured for single crystal of $[Mg(H_2O)_6][SiF_6]$. At 283 K, $(e^2Qq/h, \eta)$ of ^{2}H, averaged by fast 180° flip of water molecules, were obtained as (128 kHz, 0.72), (123 kHz, 0.82) and (106 kHz, 0.80), corresponding to three unequal water molecules in $[Mg(H_2O)_6]^{2+}$. At 338 K, $(e^2Qq/h, \eta)$ averaged further by the fast reorientation of $[Mg(H_2O)_6]^{2+}$ around the C_3 axis was obtained as (57 kHz, 0.01). In phase II, the jumping rate for the reorientation (k) and the amplitude of the rotational modulation $(\Delta\alpha)$ of $[Mg(H_2O)_6]^{2+}$ about the C_3 axis were obtained from the simulation of ^{2}H NMR spectra. The jumping rate at infinite temperature and the activation energy were estimated from the temperature dependence of k as $k_0 = 9 \times 10^{17}$ s^{-1} and $E_a = 78$ kJmol^{-1}, respectively. The II-III phase transition was found to be related with the freeze of this motion.

Key words: Nuclear Quadrupole Interaction; ^{2}H NMR; Incommensurate Phase; Rotational Modulation; Molecular Dynamics.

Introduction

Most of the $[M(H_2O)_6][SiF_6]$ type crystals undergo structural phase transitions due to the orientational order-disorder of $[M(H_2O)_6]^{2+}$ and $[SiF_6]^{2-}$ [1 - 11]. In particular, $[Mg(H_2O)_6][SiF_6]$ is known to exhibit successive phase transitions and to have five stable phases [1]. Denoting these phases as I, II, ..., V in order of decreasing temperature, phase II is an incommensurate phase. The crystal structure in phases II and IV has been investigated by diffraction methods [2 - 5]. The space group of phase IV is $P2_1/c$ with Z = 2. The structure of phase II was specified as an arrangement of domains of different octahedra orientation with overall space group $P\bar{3}$, although an analysis based on a modulated structure was not performed. The modulated structure was found by ESR spectroscopy to be a vibrational modulation of $[Mg(H_2O)_6]^{2+}$ expressed by a plane-wave nearly along the C_3 axis [1]. A further transition at 343 K was observed in the incommensurate phase [1, 7 - 9]. This transition changed a modulational amplitude discontinuously. Recently we have studied the motion of H_2O, $[Mg(H_2O)_6]^{2+}$ and $[SiF_6]^{2-}$ by spectra and T_1 of ^{1,2}H and ^{19}F NMR in the powder sample [9]. The phase transitions were found to be closely related with the motion of $[Mg(H_2O)_6]^{2+}$. However, information about the modulated structure was not obtained and is considered to be an acquired in an orientational sample. In the present work, ^{2}H NMR spectra in a single crystal were measured to study the static and dynamic structures of H_2O and $[Mg(H_2O)_6]^{2+}$ in detail. The principal components and the direction cosines of the nuclear quadrupole interaction were obtained at 283 K (phase IV) and 338 K (phase II) from the angular dependence of the ^{2}H NMR quadrupole splitting. From the spectral simulation in phase II, the rotational modulation of $[Mg(H_2O)_6]^{2+}$ was shown to exist, and the jumping rate of $[Mg(H_2O)_6]^{2+}$ was estimated. Moreover, the correlation between this motion and II-III transition was obtained.

0932–0784 / 02 / 0600–0408 $ 06.00 © Verlag der Zeitschrift für Naturforschung, Tübingen · www.znaturforsch.com

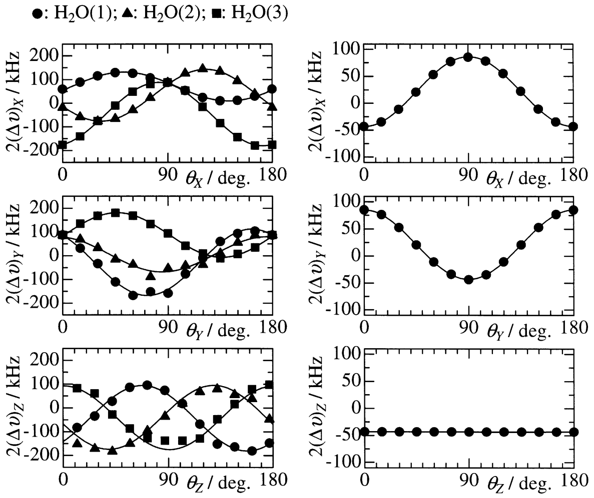

(a) $T = 283$ K (b) $T = 338$ K

Fig. 1. Angular dependences of the ^{2}H NMR quadrupole splitting, $2(\Delta\nu)$, around the X, Y, and Z axes in [Mg(H_2O)$_6$][SiF$_6$]. (a) and (b) show $2(\Delta\nu)$ at 283 K (phase IV) and 338 K (phase II), respectively. The solid lines show the theoretical curves.

Experimental

The deuterated sample was obtained by repeated recrystallization from heavy water. A single crystal of a transparent white prism elongated along the C_3 axis was obtained. It was found that the crystal Z axis is along the C_3 axis and the X and Y axes are perpendicular to the Z axis. The ^{2}H NMR spectra were measured by a CMX-300 spectrometer at 45.826 MHz. The sample was mounted on an uniaxial goniometer so as to allow rotation about a chosen axis perpendicular to the external magnetic field. A quadrupole echo sequence ($90^\circ_x - \tau - 90^\circ_y - \tau -$ acq) was used. The 90° pulse width and τ were 3.0 and 20 µs, respectively.

Results and Discussion

Figure 1(a) shows the angular dependences of the ^{2}H NMR quadrupole splitting, $2(\Delta\nu)$, around the crystal X, Y, and Z axes at 283 K (phase IV). Three $2(\Delta\nu)$ which can be attributed to three unequal water molecules in [Mg(H_2O)$_6$]$^{2+}$ were observed for each rotation. It is found that the electric field gradient (EFG) tensors for two deuterons in a water molecule are averaged by the fast 180° flip of H_2O resulting in the same tensors [9, 12] and that inversion symmetry exists for [Mg(H_2O)$_6$]$^{2+}$ at this temperature [2]. The fitting calculation for the rotation around the X axis was performed with the equation [13]

$$2(\Delta\nu)_X = \frac{3eQ}{4h}\big[V_{XX} + (V_{ZZ} - V_{YY})\cos(2\theta_X) + 2V_{YZ}\sin(2\theta_X)\big], \quad (1)$$

where θ_X is the angle between the Y axis and the external magnetic field B_0. V_{ij} $(i, j = X, Y, Z)$ are the components of the EFG tensor in the crystal fixed frame. The equations corresponding to the rotations around the Y and Z axis are obtained by cyclic permutation. All V_{ij} $(i, j = X, Y, Z)$ can be obtained by rotation around three orthogonal axes. Table 1 shows the principal values of the quadrupole interaction e^2Qq_{ii}/h $(i = x, y, z)$ and the direction cosines of the principal axes with respect to the crystal axes obtained by the diagonalization of the V_{ij} tensor. At 283 K, the deuteron quadrupole interaction parameters $(e^2Qq/h, \eta)$, averaged by the fast 180° flip of H_2O, were obtained as (128 kHz, 0.87), (124 kHz, 0.89) and (122 kHz, 0.98) for $H_2O(1)$, $H_2O(2)$ and $H_2O(3)$, respectively. Figure 1(b) shows the angular dependences of $2(\Delta\nu)$ around the X, Y and Z axes at 338 K (phase II). The Z axis is parallel to the C_3 axis of the crystal in this phase. At this temperature only one $2(\Delta\nu)$, corresponding to the EFG tensor averaged further by the fast reorientation of [Mg(H_2O)$_6$]$^{2+}$ around the C_3 axis, was observed for rotation about each crystal axis. e^2Qq_{ii}/h $(i = x, y, z)$ and the direction cosines with respect to the crystal axes at 338 K are also shown in Table 1. The EFG tensor, averaged

Table 1. The principal components and the direction cosines of the EFG tensors of deuterons in [Mg(H_2O)$_6$][SiF$_6$].

T / K		$\lvert e^2Qq_{ii}\rvert h^{-1}$ / kHz	– Direction cosines – X	Y	Z
		8	−0.0946	0.7270	0.6800
	$H_2O(1)$	120	−0.3627	0.6109	−0.7036
		128	−0.9270	−0.3132	0.2059
		6	−0.5910	−0.4104	0.6943
283	$H_2O(2)$	118	−0.3734	−0.6237	−0.6866
		124	0.7149	−0.6651	0.2154
		1	0.6945	−0.1638	0.7005
	$H_2O(3)$	121	0.0684	0.9843	0.1622
		122	−0.7162	−0.0647	0.6948
		29	0.9887	0.1492	−0.0011
338		28	−0.1493	0.9887	−0.0053
		57	0.0003	0.0054	0.9999

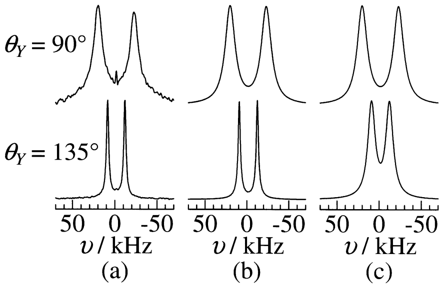

Fig. 2. ^{2}H NMR spectra of $[Mg(H_2O)_6][SiF_6]$ at θ_Y of 90° and 135°. (a) shows the observed spectra at 338 K. (b) and (c) show the simulated spectra with $k = 7.7 \times 10^5\ \mathrm{s}^{-1}$. (b) takes account of the modulated structure ($\Delta\alpha = 23°$), but (c) does not ($\Delta\alpha = 0°$). All the spectra are normalized.

by the fast reorientation of $[Mg(H_2O)_6]^{2+}$ around the C_3 axis, is axially symmetric ($\eta_{\mathrm{re}} = 0$) and has its principal z axis along the C_3 axis [12, 14]. The quadrupole coupling constant e^2Qq_{re}/h, averaged by this reorientation is given by

$$\frac{e^2Qq_{\mathrm{re}}}{h} = \frac{1}{2}\frac{e^2Qq}{h}\left(3\cos^2\beta - 1 + \eta\sin^2\beta\cos 2\gamma\right), \quad (2)$$

where $(e^2Qq/h, \eta)$ are the parameters of the non-averaged tensor. (α, β, γ) are the Euler angles for the transformation from the molecular axes to the principal axes system of the non-averaged quadrupole tensor. Assuming that the molecular axes coincide with the crystal axes in phase IV and using $(e^2Qq/h, \eta)$ = (128 kHz, 0.87) and (β, γ) = (78.1°, 226.0°), estimated from EFG tensor of the deuterons of $H_2O(1)$ obtained at 283 K, e^2Qq_{re}/h was calculated as 58 kHz. $(e^2Qq_{\mathrm{re}}/h, \eta_{\mathrm{re}})$ obtained at 338 K was (57 kHz, 0.01), and the principal z axis of the EFG tensor almost coincided with the C_3 axis. Since the experimental results agreed with the theoretical prediction, the principal components and the direction cosines obtained at 283 and 383 K are considered to be reasonable.

Figure 2(a) shows ^{2}H NMR spectra observed at 338 K. The simulation of the spectra in phase II was performed by considering the three-site jump of $[Mg(H_2O)_6]^{2+}$ in the presence of the rotational modulation of $[Mg(H_2O)_6]^{2+}$ ions along the C_3 axis, as shown in Figure 3. The site frequency ω_i is written by the second-order Wigner rotation matrix $D^{(2)*}_{nm}(\Omega)$ as [9 - 11, 15 - 18]

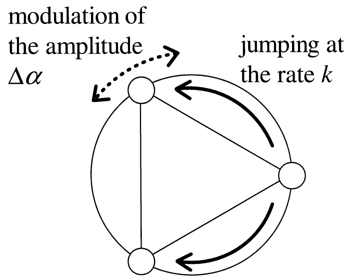

Fig. 3. Three-site jumping and rotational modulation of $[Mg(H_2O)_6]^{2+}$ about the C_3 axis. Three small circles show the water molecules on the top face of the $[Mg(H_2O)_6]^{2+}$ octahedron. The solid arrows show the possible jumps from a site. The dotted arrow shows the modulation expressed by (5).

$$\omega_i = \sqrt{\frac{3}{2}} \sum_{n,m=-2}^{2} D^{(2)*}_{0n}(\psi, \theta, \phi) D^{(2)*}_{nm}(\alpha, \beta, \gamma) T^{(2)}_{m}, \quad (3)$$

$$T^{(2)}_{0} = \sqrt{\frac{3}{8}}\frac{e^2Qq}{\hbar}, \quad T^{(2)}_{\pm 2} = \frac{\eta}{4}\frac{e^2Qq}{\hbar}, \quad (4)$$

where (ψ, θ, ϕ) are the Euler angles for the transformation from the laboratory axes to the molecular axes. The rotational phase modulation can be given as [19 - 21]

$$\alpha = \alpha_0 + \Delta\alpha\cos\zeta(x) = \alpha_0 + \Delta\alpha\cos\zeta, \quad (5)$$

where α_0 is the initial phase. $\Delta\alpha$ and $\zeta(x)$ are the amplitude and the phase angle of the rotational modulation of the $[Mg(H_2O)_6]^{2+}$ ions. x is the coordinate along the modulation axis. A plane-wave modulation was assumed for $\zeta(x)$ in the last step of (5). The values $(e^2Qq/h, \eta)$ = (128 kHz, 0.87) and (β, γ) = (78.1°, 226.0°) were used again. The frequencies of the three sites in the absence of the modulation were specified by α_0 = 50°, 170° and 290°. (θ, ϕ) is (180°, 90°) and (180°, 45°) for θ_Y of 90° and 135°, respectively. The quadrupole echo signal $G(t, \zeta)$ is written as [9, 17, 18]

$$G(t, \zeta) = \mathbf{P} \cdot \exp[\hat{\mathbf{A}}t]\exp(\hat{\mathbf{A}}\tau)\exp(\hat{\mathbf{A}}^*\tau) \cdot \mathbf{1}, \quad (6)$$

$$\hat{\mathbf{A}} = \begin{pmatrix} \mathrm{i}\omega_1 - 2k & k & k \\ k & \mathrm{i}\omega_2 - 2k & k \\ k & k & \mathrm{i}\omega_3 - 2k \end{pmatrix}. \quad (7)$$

Here, $\mathbf{1}$ is a vector written by $\mathbf{1}$ = (1, 1, 1). A vector of site population was assumed as $\mathbf{P}$ = (1/3, 1/3, 1/3).

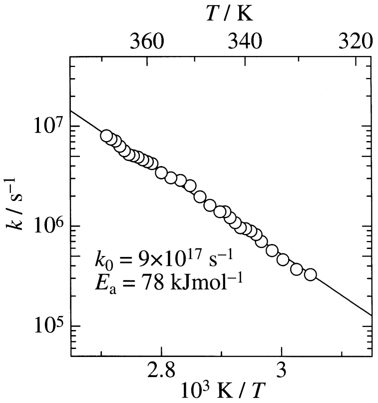

Fig. 4. Temperature dependence of the jumping rate (k) for the reorientation of $[Mg(H_2O)_6]^{2+}$ in phase II.

The signal of the sample of the single crystal is given by

$$G(t) = \int_0^{2\pi} G(t,\zeta)\mathrm{d}\zeta. \quad (8)$$

The spectrum was obtained by Fourier transform of $G(t)$. Figures 2(b) and 2(c) show the calculated spectra. At $\theta_Y = 90°$ ($C_3 \perp B_0$) we could determine the jumping rate (k) for the reorientation of $[Mg(H_2O)_6]^{2+}$ around the C_3 axis exactly, since the spectra were almost insensitive to the modulated structure. On the other hand, the spectra at $\theta_Y = 135°$ were sensitive to the modulation. The modulational amplitude ($\Delta\alpha$) could be determined by the simulation of the spectra at $\theta_Y = 135°$ using k estimated from the simulation at $\theta_Y = 90°$. In our model, the rotational modulation of $[Mg(H_2O)_6]^{2+}$ influenced on the spectra at $\theta_Y = 135°$ not to produce the 'edge singularities' [19, 20] but to reduce the linewidth. This effect can be explained as follows: The signal for the different orientation of $[Mg(H_2O)_6]^{2+}$ arising from the rotational modulation is added in (8), and the linewidth and the intensity of the spectrum transformed from each signal can be distinct owing to the reorientation of $[Mg(H_2O)_6]^{2+}$. As a consequence, the resulting spectrum is dominated by the narrower and stronger spectrum if it exists. At 338 K, k and $\Delta\alpha$ were estimated as 7.7×10^5 s^{-1} and 23°, respectively. The temperature dependence of k, obtained by the spectral simulation in phase II, is shown in Figure 4. Assuming an Arrhenius relation, k is given by

$$k = k_0 \exp(-E_a/RT), \quad (9)$$

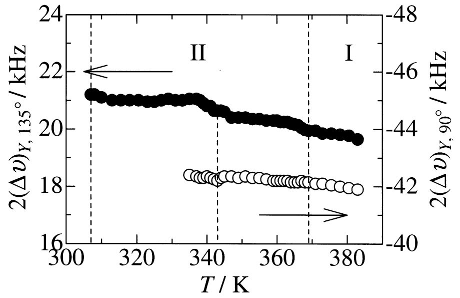

Fig. 5. Temperature dependences of the ^{2}H NMR quadrupole splitting, $2(\Delta\nu)$, in phases I and II for $[Mg(H_2O)_6][SiF_6]$. ○ and ● show $2(\Delta\nu)$ at θ_Y of 90° and 135°, respectively.

where k_0 and E_a are the jumping rate at infinite temperature and the activation energy for the reorientation of $[Mg(H_2O)_6]^{2+}$ around the C_3 axis. $k_0 = 9 \times 10^{17}$ s^{-1} and $E_a = 78$ kJmol^{-1} were obtained by fitting (9) to the temperature dependence of k. These values in the single crystal are different from those in the powder sample ($k_0 = 3 \times 10^{15}$ s^{-1} and $E_a = 62$ kJmol^{-1}), where the spectra were simulated by considering only the reorientation of $[Mg(H_2O)_6]^{2+}$ [9]. We believe that the former is better than the latter, because in this study the spectra were analyzed by separating the effect on the spectral shape of the motion of $[Mg(H_2O)_6]^{2+}$ and that of the modulated structure.

Figure 5 shows the temperature dependences of the ^{2}H NMR quadrupole splitting, $2(\Delta\nu)$, in phases I and II. Entering into phase II on heating, the spectrum changed suddenly. At $\theta_Y = 90°$ the spectrum was hardly observed below ca. 330 K in phase II because of the exchange broadening due to the reorientation of $[Mg(H_2O)_6]^{2+}$ around the C_3 axis. This shows that the II-III transition (T_c = 307 K) is closely related to the freeze of the motion of $[Mg(H_2O)_6]^{2+}$. Above ca. 330 K, the spectrum which consists of two peaks leading to one $2(\Delta\nu)$ did appear, and motional narrowing occurred with increasing temperature. At $\theta_Y = 135°$ the peaks of the spectrum were so intense even at low temperatures that we could determine $2(\Delta\nu)$. This is because the spectrum at $\theta_Y = 135°$ is dominated by not only the reorientation but the modulated structure of $[Mg(H_2O)_6]^{2+}$, as described above. A change in $2(\Delta\nu)$ due to the phase transition was observed at around 343 K. Since the change at $\theta_Y = 135°$ was larger than that at $\theta_Y = 90°$, the transition at 343 K is predicted to be related with the rotational modulation of $[Mg(H_2O)_6]^{2+}$. A large change in $2(\Delta\nu)$ due to the I-II transition was not observed. This agrees with the normal-incommensurate transition being of second order.

Conclusions

We analyzed the ^{2}H NMR spectra in single crystal $[Mg(H_2O)_6][SiF_6]$ and found for the first time the rotational modulation of $[Mg(H_2O)_6]^{2+}$ along the C_3 axis in phase II. Taking account of this modulation, the jumping rate for the reorientation of $[Mg(H_2O)_6]^{2+}$ around the C_3 axis was estimated accurately. The II-III transition was found to be related closely with the freeze of this reorientation. The correlation between the transition at 343 K and the rotational modulation of $[Mg(H_2O)_6]^{2+}$ was predicted.

[1] M. Suhara, T. Bandoh, T. Kitai, T. Kobayashi, and H. Katsuda, Phase Transitions **37**, 111 (1992).

[2] S. Syoyama and K. Osaki, Acta Cryst. **B28**, 2626 (1972).

[3] G. Jehano and F. Varret, Acta Cryst. **A31**, 857 (1975).

[4] G. Chevrier and G. Jehano, Acta Cryst. **A35**, 912 (1979).

[5] G. Chevrier, J. Solid State Chem. **99**, 276 (1992).

[6] A. Kassiba, R. Hrabanski, D. Bonhomme, and A. Hader, J. Phys.: Condens. Matter **7**, 3339 (1995).

[7] A. M. Ziatdinov, V. G. Kuryavyi, and R. L. Davidovich, Sov. Phys. Solid State **27**, 1288 (1985).

[8] A. M. Ziatdinov, V. G. Kuryavyi, and R. L. Davidovich, Sov. Phys. Solid State **30**, 1833 (1988).

[9] J. Kimura, T. Fukase, M. Mizuno, and M. Suhara, Z. Naturforsch. **53a**, 453 (1998).

[10] T. Iijima, M. Mizuno, and M. Suhara, Z. Naturforsch. **55a**, 173 (2000).

[11] M. Mizuno, T. Iijima, and M. Suhara, J. Phys.: Condens. Matter **12**, 7261 (2000).

[12] T. G. Barnes, Advances in Nuclear Quadrupole Resonance, vol. 1, (ed. by J. A. S. Smith, Heyden, London 1974, p. 335).

[13] G. M. Volkoff, Can. J. Phys. **31**, 820 (1953).

[14] K. Schmidt-Rohr, and H. W. Spiess, Multidimensional Solid-State NMR and Polymers, (Academic Press: London 1994).

[15] M. E. Rose, Elementary Theory of Angular Momentum, John Wiley, New York 1957).

[16] R. R. Vold, Nuclear Magnetic Resonance Probes of Molecular Dynamics, (ed. by R. Tycko, Kluwer Academic Publishers 1994, p. 27).

[17] M. S. Greenfield, A. D. Ronemus, R. L. Vold, R. R. Vold, P. D. Ellis, and T. E. Raidy, J. Magn. Reson. **72**, 89 (1987).

[18] M. Mizuno, T. Iijima, K. Orii, and M. Suhara, Z. Naturforsch. **55a**, 178 (2000).

[19] R. Blinc, Phys. Rep. **79**, 331 (1981).

[20] R. Blinc, I. P. Aleksandrova, A. S. Chaves, F. Milia, V. Rutar, J. Seliger, B. Topic, and S. Zumer, J. Phys. C: Solid State Phys. **15**, 547 (1982).

[21] M. Suhara and T. Kobayashi, Phase Transitions **27**, 51 (1990).